Étude de l'écoulement turbulent autour d'un turbo-voile

Ouahiba Guerri, Erwan Liberge, Aziz Hamdouni

Study of the turbulent flow around a turbosail

O. Guerri[a], E. Liberge[a], A. Hamdouni[a]

a. *LaSIE, Université de La Rochelle, Avenue Michel Crépeau, 17042 La Rochelle Cedex 1, France*

Résumé :

Cette étude est basée sur la simulation numérique de l'écoulement turbulent autour d'une turbo-voile, un profil épais équipé d'une grille d'aspiration. Les équations instationnaires de Navier Stokes sont formulées pour un fluide incompressible et résolues pour un nombre de Reynolds basé sur la corde du profil $Re = 10^5$. Les simulations sont d'abord effectuées pour un profil sans grille, en faisant abstraction de la zone fluide à l'intérieur de la turbo-voile. Cette dernière est alors placée sous une incidence nulle puis sous un angle d'attaque de 15°. Différents modèles de turbulence sont appliqués : le modèle $v2f$, le modèle R_{ij} SSG et le modèle LES dynamique. Ensuite, c'est le cas de la turbo-voile équipée d'une grille avec aspiration qui est étudié. Pour cette dernière configuration, les calculs sont exécutés avec le modèle R_{ij} SSG. Les résultats obtenus montrent l'influence de quelques caractéristiques de la grille sur les performances du profil.

Abstract :

This study is based on numerical simulation of turbulent flow around a turbo sail, a bluff body equipped with suction grid. The unsteady Navier-Stokes equations are expessed for an incompressible fluid and solved for a Reynolds number based on the profile chord $Re = 10^5$. Simulations are first performed for the profile without suction grid, ignoring the fluid area inside the turbo sail. This profile is set at zero incidence and at an angle of attack of 15°. Three turbulence models are applied : the dynamic LES model, the $v2f$ model and the R_{ij} SSG. Then the case of the turbo-sail fitted with a suction grid is studied. For this configuration, computations are performed with the R_{ij} SSG turbulence model. The obtained results show the influence of some grid characteristic on profile performances.

Mots clefs : turbosail ; RANS ; LES

1 Introduction

The work presented here focuses on the flow control around a thick profile, the aim being the improvement of aerodynamic profile performance. As already mentionned by [11] and other [5], there are different techniques to control the boundary layer, passive or active [6, 7], based on the blowing or suction or on synthetic jets [2]. The control technique applied here is the suction of the boundary layer which result in drag reduction.

The studied device is the turbosail, a profile intended for ship propulsion, similar to that used on the Alcyone [10]. The section profile has an ovoid shape with a prolonged spoiler and it is equipped with an intake grid on the upper surface, all along the span. The turbosail is hollow, the interior being of cylindrical shape. The air suction is carried by the circular base.

This study is carried out by numerical simulation of the flow around the profile. The methodology as well as the obtained results are presented in the next sections.

2 Numerical approach

It is assumed that local velocities and Mach numbers are low so that the compressibility effects are neglected. The flow is modeled using an incompressible Navier Stokes solver, assuming a fully turbulent

flow. Three turbulence models are compared : an eddy viscosity model, $v2f$, a Reynolds Stress transport Model (RSM), R_{ij} SSG and a dynamic LES model. The model equations can be described as follows :

Let $\Omega \subset R^3$ a $3D$ spatial domain occupied by the fluid and x_i the Cartesian coordinates of a point of Ω. The incompressible Navier Stokes equations are based on pressure-velocity formulation and expressed in the general Cartesian tensor as :

– Mass equation

$$\frac{\partial u_i}{\partial x_j} = 0 \tag{1}$$

– Momentum equations

$$\rho \frac{\partial u_i}{\partial t} + \rho \frac{\partial u_i\, u_j}{\partial x_j} = -\frac{\partial p}{\partial x_i} + 2\,\frac{\partial\,(\nu\, S_{ij})}{\partial x_j} - \frac{\partial \tau_{ij}}{\partial x_j} \tag{2}$$

with

$$S_{ij} = \frac{1}{2}\left(\frac{\partial u_i}{\partial x_j} + \frac{\partial u_j}{\partial x_i}\right) \qquad \textit{and} \qquad \tau_{ij} = 2\nu_t S_{ij} + \frac{1}{3}\tau_{kk}\delta_{ij}$$

where u_i and p are respectively, the time-averaged velocity components and the pressure for RANS models, or the filtered velocity components and the pressure for the LES model. ν_t is the turbulent viscosity provided by the RANS model. As for the LES one, ν_t is the subgrid scale viscosity. δ_{ij} is the Kronecker coefficient. ρ is the fluid density and ν is the fluid kinematic viscosity.

2.1 Turbulence modeling

The $v2f$ model is based on three transport equations for k, ε and $\overline{v}^2$ (the normal component of the Reynolds stress tensor) and on an elliptic equation for f, the source term of $\overline{v}^2$. Different versions of the $v2f$ model have been developed since it was introduced by Durbin. The model used in this work was proposed by Laurence et al. [9]. It is based on a change of variable from $\overline{v}^2$ to $\varphi = \overline{v}^2/k$ that lead to, a boundary value problem with homogeneous boundary conditions, fixed-sign source terms [9] and a modified equation for f being $\overline{f}$. Far from the wall, it is assumed that the turbulence is isotropic and the $k-\varepsilon$ equations are then applied.

The R_{ij} SSG model is quadratically non linear in the anisotropy tensor [13]. This model uses a Reynolds stress approach that improve the pressure-rate-of strain in the Reynolds stress equations by taking into account the non-linear return to isotropy. According to Basara et al. [3] the R_{ij} SSG model provides accurate results for a wide range of applications as recirculating flows or vortex shedding calculations.

In the dynamic LES model, the Smagorinsky constant varies in space and time. The version used in these simulations is the Germano model based on a least square method.

2.2 Boundary conditions

Boundary conditions for RANS computations. Inlet conditions specified for RANS computations are U_∞, the free stream velocity, k_∞, the free stream turbulence energy and ε_∞, the dissipation rate of turbulence defined as : $k_\infty = 1.5\,U_\infty^2\,I^2$ and $\varepsilon_\infty = 10\,C_\mu\,k_\infty^{3/2}/(\kappa\,L_{ref})$ where I is the turbulence intensity, $L_{ref} = c$ is the reference chord lenght, C_μ and κ are constants ($C_\mu = 0.9$ and $\kappa = 0.42$).

A wall function is applied with the R_{ij} SSG model, a high Reynolds numbers turbulence model. The law used is a two velocity model that involve the friction velocity of the fluid at the wall, u^*, and a friction velocity u_k, which is a function of the kinetic energy of turbulence k.

Inlet conditions for LES computations. The numerous work related to boundary conditions in LES calculation [8, 12] show that the definition of appropriate boundary conditions is not always obvious, in particular for inlet condition. A review of some applied techniques is presented by Tabor and Baba-Ahmadi [14]. In our case, we used the Synthetic Eddy Method (SEM) of Jarrin et al. [8]. The inlet flow field is decomposed as a finite sum of spin eddies of which size is equal to the turbulent length scale. According to Jarrin et al. [8], this technique reproduces the best structures of the flow. Similar comments were reported by Patil et al. [12] who have applied this technique for a backward facing step.

2.3 Algorithm and schemes

All simulations are performed using code_Saturne *(version 2.3)*. The equations are solved by the finite volume method with a fractional time step integration, similar to SIMPLEC algorithm. SOLU, a second order UPWIND scheme is applied for the spatial discretization of momentum equations. Equations for k and ε are discretized using the UPWIND scheme. The finite volume method implemented in code_Saturne is formulated for non-staggered and unstructured grids. An iterative method is applied to calculate the gradients at the interfaces [1]. For RANS calculations, a first order implicit time integration scheme is used. Second order schemes are used for LES computations.

3 Results

The turbosail is set at the center of an H-domain which extend for a distance equivalent to $5\,L_{ref}$ upstream and $30\,L_{ref}$ downstream. South and North domain boundaries are located at about $\pm 12.5\,L_{ref}$. The turbosail span is equal to $4\,L_{ref}$ and upper boundary is located at $4\,L_{ref}$.

The governing equations are solved for a Reynolds number based on the chord of the profile $Re = 10^5$. First, calculations are performed ignoring the fluid area inside the turbosail, without suction and grille. The turbosail is then set at fixed incidence. Thereafter, the profile is equipped with suction and grid all along the span.

3.1 Profile without suction

RANS computations. Two computationnal grids of about $3\,10^6$ cells are built for RANS models. The two grids are similar. They are both of hybrid type and generated by block. But they differ by the value of y_0, the first row height of cells around the turbosail. y_0 is chosen so that the adimensionnal height $y^+ \approx 1$ for the $v2f$ computations and $y^+ \approx 20$ to 180 for the R_{ij} SSG computations. These RANS computations are performed for the turbosail set at two fixed angle of attack, 0° and 15° but only results are given for the profile at 0°.

The velocity contours obtained with both turbulence models at two time steps $t^* = U_\infty\, t/c$ are shown on figure 1. The maximal velocities found are $2.0\,U_\infty$ for the SSG model and $1.7\,U_\infty$ for the $v2f$ model. Higher acceleration of the flow is then obtained with the R_{ij} SSG model. As for the $v2f$ model, a larger accelerated fluid zone is found. Separation occurs at about 110° on the upper surface and shedding vortices are observed in the wake. The flow structures of the wake seem similar for both models (Figure 1 (a) to (d)) however, with the $v2f$ model, the vortices are mixed downstream the turbosail in the near wake Figure (1 (e)). The R_{ij} SSG model shows that the two pairs of vortices are mixed also in the wake but small spinning vortices still remain. (Figure 1 (f)). Spoiler causes asymmetric wake flow that is not found with the $v2f$ model. These results are also shown by the curves of lift and drag coefficients depicted on figure 2. The $v2f$ model shows that both lift and drag coefficients are varying periodically ; Moreover a small periodic secondary oscillation is observed for the drag coefficient. The R_{ij} SSG model shows that both lift and drag curves have a double oscillation, one with a small amplitude and low period and the second with a higher amplitude and longer period. The small oscillations are attributed to the spoiler influence and the larger ones to the vortex created by the flow separation on the extrados. Similar values are found for the drag coefficient, which is not the case for the average lift coffecient.

Flow patterns found with the R_{ij} SSG model are similar to those found with other computations performed with the low Reynolds number R_{ij} EBRSM model (not shown here) but average values of the lift and drag coefficients are close to those obtained with $v2f$ model. This could be explained as follows : boundary layer is well resolved by the low Reynolds number $v2f$ model but this is not the case for areas away from the wall and mainly the wake. In these zones, the flow is better resolved by the R_{ij} SSG model. However, with this high Reynolds model, boundary layer flow is not accurately resolved especially when evaluating pressure forces. As the wake flow is well predicted by this model, the drag force calculation is improved.

LES computations. Two computationnal grids are built for LES simulations. The first one is composed of about $12\,10^6$ cells, with 60 elements on the span and the second one is composed of more than

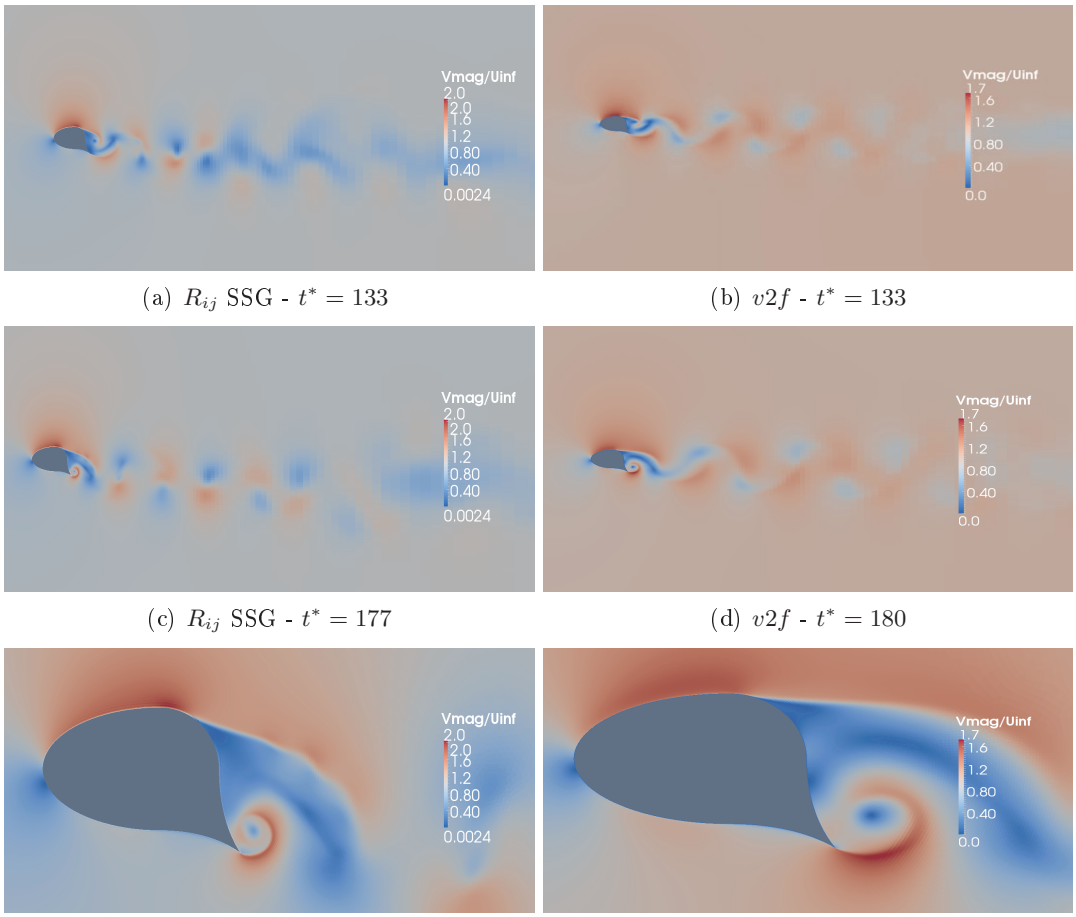

(a) R_{ij} SSG - $t^* = 133$ (b) $v2f$ - $t^* = 133$

(c) R_{ij} SSG - $t^* = 177$ (d) $v2f$ - $t^* = 180$

(e) R_{ij} SSG - $t^* = 177$ - In the vicinity of the airfoil (f) $v2f$ - $t^* = 180$ - In the vicinity of the airfoil

FIGURE 1 – Velocity magnitude contours around the turbosail set at $\alpha = 0°$ incidence - $v2f$ and R_{ij} SSG models

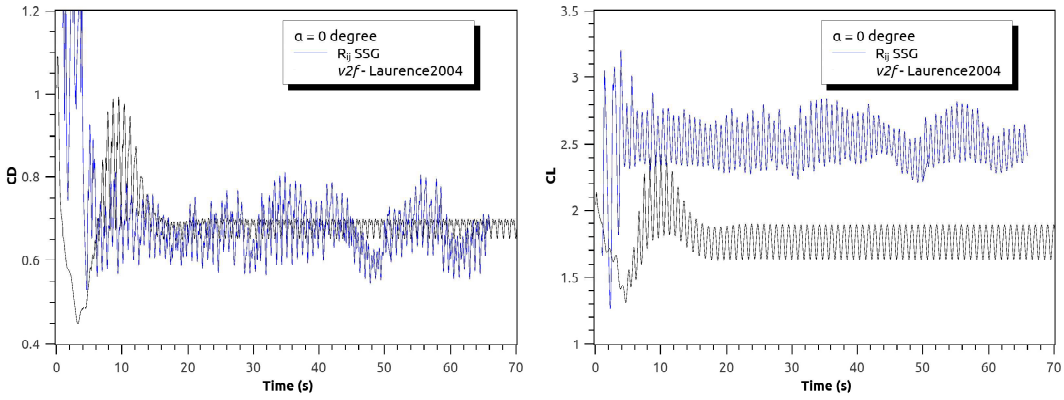

(a) CD-RANS-$\alpha = 0°$ (b) CL-RANS-$\alpha = 0°$

FIGURE 2 – Temporal variations of drag and lift coefficients for the turbosail set at $\alpha = 0°$ incidence - RANS models

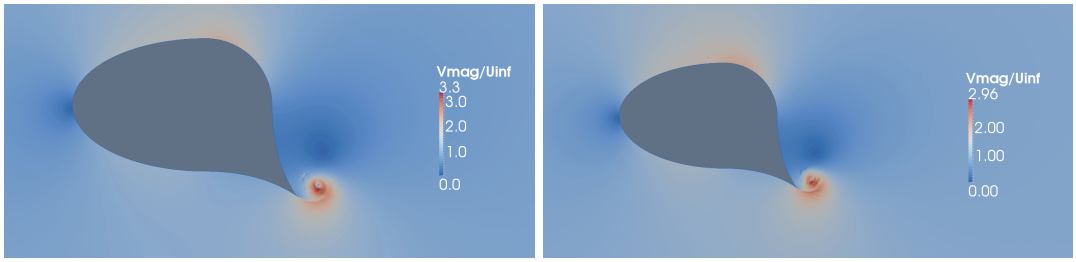

(a) Mesh1 - $t^* = 6.58$ (b) Mesh2 - $t^* = 6.56$

FIGURE 3 – Contours of velocity magnitude obtained with LES computations

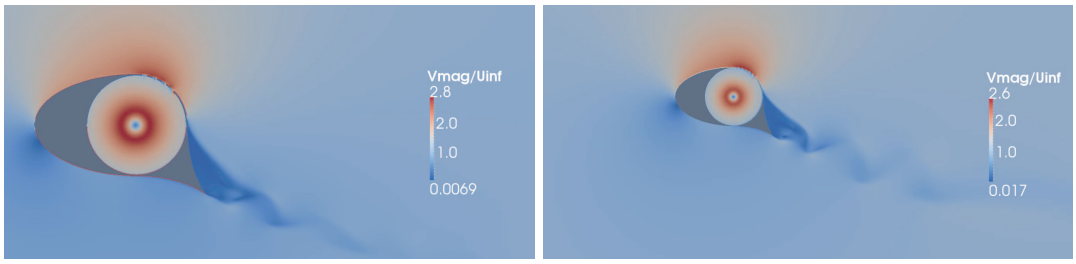

(a) case 484 (b) case 486

FIGURE 4 – Velocity contours around the turbosail with suction

$22.5\,10^6$ cells with 120 elements along the span. In both grids, the spacing around the turbosail are $\delta s/c \approx 3\,10^{-3}$ and $y^+ \approx 1$. This is a coarser LES simulations in the spanwise direction but nevertheless, it is expected that the main physical structures will be captured.

Similar results are achieved with both computationnal grids. The contours of velocity magnitude (Figure 3) show the begining of the rotating vortex creation downstream the spoiler.

3.2 Profile with suction

For the turbosail equipped with grille and suction, two configurations are considered. In both cases, the grille extends over 48°. The influence of the slots number is compared : the first grille has 4 slots (case 484) and the second one has 6 slots (case 486). These computations are performed with the R_{ij} SSG turbulence model.

Velocity contours around both turbosails with suction are represented on figure 4. The figure shows that the massive turbulent separation on the extrados does not occur. It is laminarized and delayed near the trailing edge, on the spoiler. It is also shown that the vortex sheddings are suppressed by suction. The flow is accelerated in the neighborhood of the suction grille.

The resulting lift and drag coefficients are depicted on figures 5. Comparing these results with those obtained for the turbosail without suction, it is found a decrease of the drag coefficient and an increase of the lift one. Higher lift coefficient is found for the 4 slots grille, however the 6 slots grille have a higher C_L/C_D ratio. Thus, a better performance is obtained with the 6 slots grille (case 486).

4 Conclusion

Turbulent fluid flow computations have been performed for a turbosail with suction. First, three turbulence models have been applied for a profile without suction, an eddy viscosity model, a RSM model and a dynamic LES model. Similar flow patterns are obtained with both RANS models however lift coefficients are differents. Then the influence of the suction on the profile performance is considered. It is found that performance are improved and that better lift to drag ratio is obtained when the slots number increases from 4 to 6, for a given grille extend. Moreover, vortex sheddings are suppressed by the suction. It is thus expected that vortex induced vibrations will not occured.

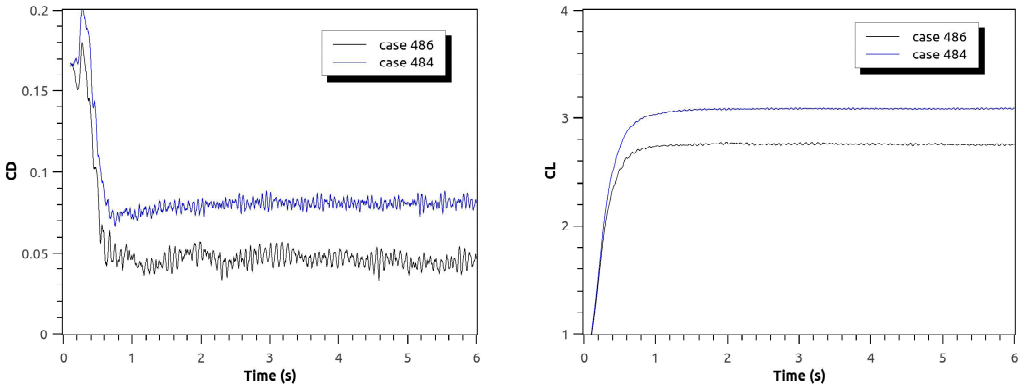

(a) Drag coefficient (b) Lift coefficient

FIGURE 5 – Temporal variations of drag and lift coefficients for turbosail with suction - case_484 and case_486

Acknowledgements The authors kindly acknowledge financial support from FEDER for this work.

Références

[1] Archambeau, F., Méchitoua, N., Sakiz, M. 2004 Code_Saturne : a Finite Volume Code for the Computation of Turbulent Incompressible Flows - Industrial Applications. *International Journal on Finite Volumes*, **1** 1-62

[2] Amitay, M., Glezer, A. 2002 Controlled transients of flow reattachment over stalled airfoils *International Journal of Heat and Fluid Flow* **23** 690-699

[3] Basara, B., Bachier, G., Schiffermuller, H. 1997 Calculation of vortex shedding from bluff bodies with the reynolds-stress model

[4] Durbin, P.A. 1991 Near-wall turbulence closure modelling without damping functions. *J. Theor. Comput. Fluid Dyn.* **3** 1-13

[5] Fournier, G., Pellerin, S., Ta Phuoc, L. 2005 Contrôle par rotation ou par aspiration de l'écoulement autour d'un cylindre calculé par Simulation des Grandes Échelles *C. R. Mecanique* **333** 273-278

[6] Godard, G., Stanislas, M. 2006 Control of a decelerating boundary layer. Part 1 : Optimization of passive vortex generators *Aerospace Science and Technology* **10** 181-191

[7] Godard, G., Foucaut, J.M., Stanislas, M. 2006 Control of a decelerating boundary layer. Part 2 : Optimization of slotted jets vortex generators *Aerospace Science and Technology* **10** 394-400

[8] Jarrin, N., Benhamadouche, S., Laurence, D., Prosser, R. 2006 A synthetic-eddy-method for generating inflow conditions for large-eddy simulations *International Journal of Heat and Fluid Flow* **27** 585-593

[9] Laurence, D.R. and Uribe, J.C. and Utyuzhnikov, S.V., 2004 A Robust Formulation of the $v2-f$ Model. *Flow, Turbulence and Combustion* **73** 169-185

[10] Malavard, L. 1984 Un nouveau propulseur éolien de navire *La vie des sciences, C. R. 1* **1** 57-72

[11] Muddada, S., Patnaik, B.S.V. 2010 An active flow control strategy for the suppression of vortex structures behind a circular cylinder *European Journal of Mechanics B/Fluids* **29** 93-104

[12] Patil,S., Tafti, D. 2012 Wall modeled large eddy simulations of complex high Reynolds number flows with synthetic inlet turbulence *International Journal of Heat and Fluid Flow* **33** 9-21

[13] Speziale, C.G., Sarkar, S. and Gatski, T.B. 1991 Modeling the pressure-strain correlation of turbulence : An invariant dynamical systems approach *J. Fluid Mech.* **227** 245-272

[14] Tabor, G.R., Baba-Ahmadi, M.H. 2010 Inlet conditions for large eddy simulation : A review *Computers & Fluids* **39** 553-567